UDC 539.3

TUNING OF VIBRO-IMPACT NONLINEAR ENERGY SINKS UNDER CHANGING STRUCTURAL PARAMETERS. PART 1

P.P. Lizunov

O.S. Pogorelova

T.G. Postnikova

Kyiv National University of Construction and Architecture

DOI: 10.32347/2410-2547.2025.114.11-22

It is shown how tuning of vibro-impact nonlinearenergy sinks to appropriate structural parameters can improve their efficiency over wider range of these parameters. Unusual "strange" values of optimized parameters for low-mass dampers (very large clearance and small damping coefficient) and narrow areas of bilateral impacts persist also at different structural parameter values.

Keywords:nonlinear energy sink, damper, vibro-impact, optimized parameters, efficiency, bilateral impacts.

1. Introduction

The nonlinear energy sinks (NESs) are relatively new passive vibration control devices that are designed to mitigate high-amplitude and high-velocity vibrations that often endanger structures and machines. They have a significantly nonlinear connection with the primary structure (PS) and were proposed after extensive discussion and application of linear passive vibration control devices. The global scientific literature indicates that linear attachments such as Tuned Mass Dampers (TMDs) operate efficiently in the narrowband frequency range, where their performance degrades with any changes in frequency content in the structure and the TMD itself. In [1], the authors note that unlike TMDs, the NESs are dynamical vibration absorbers that achieve vibration suppression for wide range of frequency-energy levels. Due to the strong nonlinearity, NESs can realize broadband targeted energy transfer (TET) and hence reduce the primary structure (PS) energy. Thus, the NESs provide more effective response mitigation, without the necessity of adding more damping [2].

The scientific literature provides comprehensive reviews of modern studies on NESs [1, 3–6]. Among many proposed and discussed types, a notable place is occupied by the impact based, i.e., vibro-impact NESs. A comprehensive review of the VI NESs can be found in [1]. The authors, referring to numerous works by the reputable authors, describe the design, analysis and applications of impact-based NESs, advantages of VI NESs, realization and models. The authors state that VI NESs, "when properly designed can act as the most effective NESs for shock and seismic energy absorption and dissipation even at severe loadings"; and the SSVI type was found of robust performance.

In many works, the authors focus on the effect of VI NES physical parameters such as clearance, mass, stiffness and coefficient of restitution on the energy dissipated and optimize these parameters. For example, in a resent paper [7], the authors, studying the dynamics of the system with double-sided VI NES with a ball in a cavity, investigate the influence of the clearance and contact stiffness on the response regimes. However, in [2], the authors, considering the system under seismic loading, do not optimize the damper mass, but construct separate contour plots for several different mass ratios when the primary structure has low damping, moderate damping, high damping, and very high damping. We also believe that damper mass should not be optimized, it should be pre-selected and other parameters should be optimized for each selected mass separately. In our previous works [8, 9], we have shown that low-mass VI NESs (mass ratio 1 and 2%) can provide good mitigation of the primary

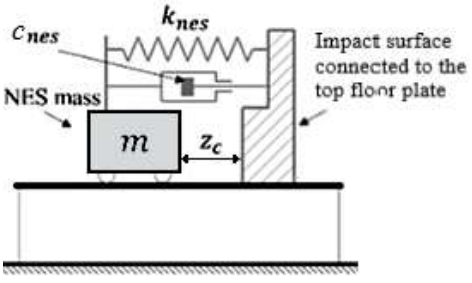

Fig.1. Schematic illustration of SSVI NES coupled to a single-story primary structure

ISSN 2410-2547
Опір матеріалів і теорія споруд/Strength of Materials and Theory of Structures. 2025. № 114

structure vibrations, but their optimized parameters acquire unusual “strange” values, namely, a huge clearance and a very small damping coefficient. In addition, the areas of bilateral damper impacts are narrow. In the present paper, we show that these phenomena are also true for other structural parameters, in particular, they persist when the primary structure damping is changed. In our next paper (Part II), we will follow these phenomena when the primary structure stiffness and the amplitude of the exciting force are varied.

Finally, it is worth noting. We use the scheme for SSVI NES shown in Fig. 2, which is given in numerous authoritative works. However, this scheme provides bilateral impacts from two sides, both directly on the primary structure and on the rigidly coupled obstacle. We have shown this in our previous works and show it in the present paper. From this point of view, the scheme given in review [1] (Fig. 1) is more in line with the name of the single-sided VI NES with obstacle impacts on one side only.

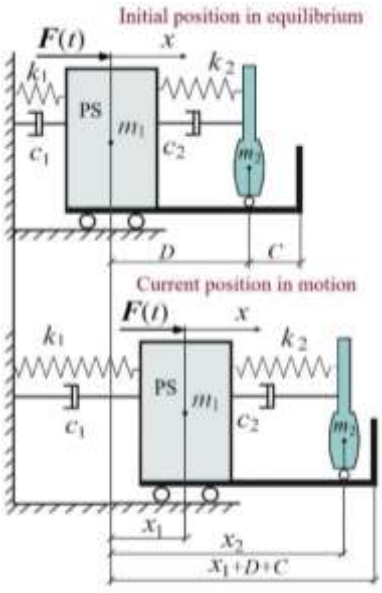

Fig. 2. Conceptual scheme of asymmetric single-sided VI NES

Thus, the goals of this paper are as follows:

- to show the influence of the VI NES tuning to the structural parameters, in particular,
to the PS damping, on their efficiency;
- to show that the VI NES attachment can replace the additional PS damping;
- to show that unusual “strange” values of the optimized parameters for the low-mass VI NES (very large clearance and small damping coefficient) and narrow areas of bilateral impacts persist also at different structural parameter values.

2. Model description and governing equations

In this paper, we study the dynamic behavior of a non-smooth strongly nonlinear vibro-impact system consisting of a primary structure (PS) and a coupled single-sided vibro-impact nonlinear energy sink (SSVI NES), which may be referred to as a vibro-impact damper. The scheme of the SSVI NES (Fig. 2) was chosen in accordance with numerous works in the scientific literature [10, 11, 12]. The primary structure is a heavy linear oscillator of mass m_1 connected to a fixed wall by a linear spring k_1 and a damper c_1, to which an obstacle is rigidly connected. The light-weight asymmetric single-sided VI NES of mass m_2 is coupled to the PS by a linear spring k_2 and a damper c_2; $m_2 << m_1$. The harmonic exciting force $F(t)$ with period T acts on the PS

$$F(t) = \mathrm{P}\cos(\omega t + \varphi_0), \quad P = 800\,\mathrm{N}, \quad T = 2\pi/\omega. \tag{1}$$

During operation, VI NES makes repeated impacts both on the PS directly and on the obstacle.

We chose the impact rule, i.e., the impact modeling method, according to the quasi-static Hertz’s contact theory [13] after examining this problem in our previous works [14]. An interactive contact nonlinear force that acts only during an impact, which has a specific duration, simulates an impact.

$$F_{con}(z) = K[z(t)]^{3/2}. \tag{2}$$

The coefficient K characterizes the mechanical and geometric properties of the colliding surfaces. It differs for the damper impacts on the PS directly and on the obstacle, since different surfaces are involved in these impacts.

When impacting the PS directly

$$K_1 = \frac{4}{3}\frac{q_1}{(\delta_1+\delta_2)\sqrt{A_1+B_1}}, \qquad \delta_1 = \frac{1-\nu_1^2}{E_1\pi},\ \delta_2 = \frac{1-\nu_2^2}{E_2\pi}.$$

When impacting the obstacle

$$K_2 = \frac{4}{3}\frac{q_2}{(\delta_3+\delta_4)\sqrt{A_2+B_2}}, \qquad \delta_3 = \frac{1-\nu_3^2}{E_3\pi},\ \delta_4 = \frac{1-\nu_4^2}{E_4\pi}. \tag{3}$$

The Young's moduli of elasticity for all surfaces E_1, E_2, E_3, E_4 and Poisson's ratios $\nu_1, \nu_2, \nu_3, \nu_4$ are the mechanical characteristics of colliding surfaces. The values E_1 and ν_1 characterize the contact surface of the PS; the values E_2 and ν_2 – the contact surface of the obstacle; the values E_2, E_4 and ν_2, ν_4 – the left and right contact surfaces of the vibro-impact damper. The constants A_1, A_2, B_1, B_2, q_1, q_2 are the geometrical characteristics of colliding surfaces; they are calculated according to the known table [13] depending on the type of contact surfaces. To use this table, we assume that the damper surfaces, both left and right, are spherical with large radii R_1 and R_2, and the contact surfaces of the primary structure and the obstacle are flat. Then $A_1 = B_1 = 1/(2R_1)$, $A_2 = B_2 = 1/(2R_2)$. We set $A_1 = A_2 = B_1 = B_2 = 0.5\,\text{m}^{-1}$, $q_1 = q_2 = 0.319$ as in the collision of a plane and a sphere. Thus, this simulation method makes it possible to calculate the contact forces and evaluate the influence of collision surface characteristics.

In formula (2), $z(t)$ is the colliding body rapprochement in the contact zone due to local deformations allowed by Hertz's law. The contact conditions are formulated by means of the Signorini's contact condition as the following: the impacts occur when

$$\begin{aligned} &x_1 \ge x_2, && \text{that is, } x_1 - x_2 \ge 0 \text{ for direct impacts on the PS;} \\ &&& \text{then } z_1 = x_1 - x_2 \\ &x_2 \ge x_1 + (D + C), && \text{that is, } x_2 - x_1 - (D + C) \ge 0 \text{ for impacts on an obstacle;} \\ &&& \text{then } z_2 = x_2 - x_1 - (D + C). \end{aligned} \tag{4}$$

Distance D and clearance C are shown in Fig. 2. Combining the Signorini contact conditions and the Hertz contact law, and using discontinuous Heaviside step function to "activate" the contact forces, we write the motion equations for this system as follows:

$$\begin{aligned} m_1\ddot{x}_1 + c_1\dot{x}_1 + k_1x_1 - c_2(\dot{x}_2 - \dot{x}_1) - k_2(x_2 - x_1 - D) &= F(t) - H(z_1)F_{con}(z_1) + H(z_2)F_{con}(z_2), \\ m_2\ddot{x}_2 + c_2(\dot{x}_2 - \dot{x}_1) + k_2(x_2 - x_1 - D) &= H(z_1)F_{con}(z_1) - H(z_2)F_{con}(z_2). \end{aligned} \tag{5}$$

The initial conditions are:

$$x_1(0) = 0,\ x_2(0) = D, \dot{x}_1(0) = \dot{x}_2(0) = 0,\ \varphi_0 = 0.$$

The presence of the discontinuous Heaviside step function $H(z)$ in the motion equations (5) makes the set of the Ordinary Differential Equations (ODE) stiff one. Stiff solvers from the *Matlab* platform can integrate the stiff sets of ODE. They provide the variable integration step and make it extremely small at the impact points. We use the solver *ode23s*.

The VI NESs are designed to mitigate the PS vibrations, that is, to reduce the total PS energy, which is calculated by the well-known formula, where $x_1(t)$ and $\dot{x}_1(t)$ are the results of integration of the set (5):

$$E_{1total}(t) = E_{1kinetic}(t) + E_{1poten}(t) = \frac{m_1\dot{x}_1(t)^2 + k_1x_1(t)^2}{2}. \tag{6}$$

When optimizing the damper parameters, its maximum is chosen as the objective function.

In this paper, some PS parameters are pre-selected

$$m_1 = 1000 \text{ kg},\ k_1 = 3.95 \cdot 10^4 \text{ N/m},\ E_1 = E_3 = 2.1 \cdot 10^{11} \text{ N/m}^2,\ \nu_1 = \nu_3 = 0.3.$$

The PS damping c_1 changes; this paper studies how these changes affect the system dynamics and damper efficiency. In our previous works [15], we have found that the softer impacts between the damper and the barriers are preferable and provide the better results, so we have chosen:

$$E_2 = 2.21 \cdot 10^7 \text{N/m}^2,\ E_4 = 2.05 \cdot 10^7 \text{N/m}^2,\ \nu_2 = \nu_4 = 0.4.$$

3. Changing the primary structure damping c_1

In this section, we consider the SSVI NESs of mass m_2=20 kg coupled to the PS with different damping c_1. How do their efficiency and system dynamic behavior change when the PS damping is changed?

ISSN 2410-2547
Опір матеріалів і теорія споруд/Strength of Materials and Theory of Structures. 2025. № 114

3.1. System behavior during optimization of damper parameters at PS damping $c_1 = 452\,\mathrm{N\cdot s/m}$

In this section, the SSVI NES was tuned to the PS damping c_1=452 N·s/m, that is, its optimal design was found for the PS with this damping. It is presented in Table 1.

Table 1

Parameters of VI NES optimized when PS damping was c_1=452 N·s/m

m_2, kg	k_2, N/m	c_2, N·s/m	C, m	D, m
20	198	36.0	0.871	0.109

These parameters have large clearance C and small damping coefficient c_2. The area of bilateral impacts on the PS directly and on the obstacle is narrow and located near the resonance (Fig. 3). The regions of unilateral direct damper impacts on the PS are wider.

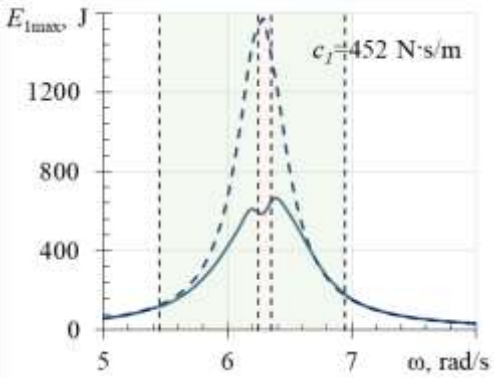

Fig. 3. The areas of bilateral (pink) and unilateral (light-green) impacts for SSVI NES with mass m_2=20 kg, whose parameters were optimized for c_1=452 N·s/m, depending on the exciting force frequency

One of the most important advantages of NESs over linear dampers is the preservation of PS vibration mitigation efficiency over a relatively broad range of the energy-frequency domain.Fig.4 demonstrates this phenomenon. It shows similar high efficiency in reducing the maximum PS energy E_{1max} despite the change in the PS damping c_1. The dashed curves show the PS energy without damper.

The same results are detailed in Table 2, in which the PS energy reduction is given as a percentage. According to the theory of targeted energy transfer (TET), the NES, due to its nonlinearity, takes away some of the PS energy, thus reducing it. Therefore, we give the values of the maximum damper energy E_{2max} in Table 2, Table 3, and Table 5.

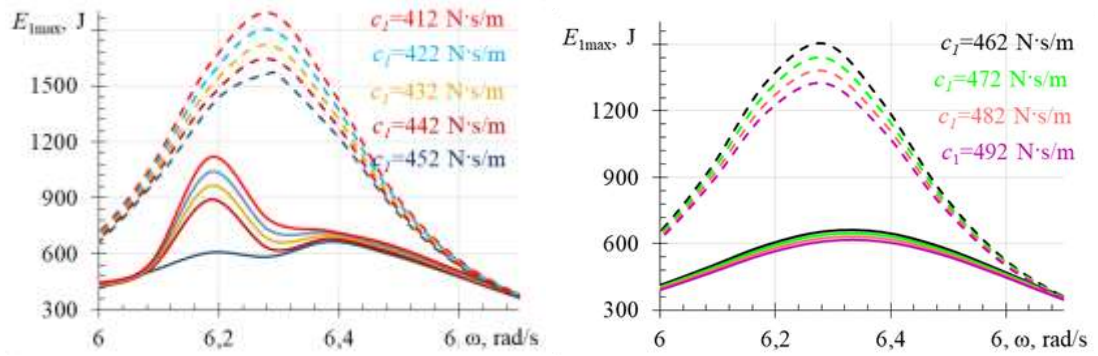

(a) (b)

Fig. 4. The reduction of maximum PS energy with attached SSVI NES when changing the PS damping c_1: (a) for c_1=412, 422, 432, 442, 452 N·s/m; (b) for c_1=462, 472, 482, 492 N·s/m

When the structural parameters are varied over a wider range, the VI NES performance is maintained but degraded. Fig. 5 shows the maximum total mechanical energy of the PS E_{1max} for four values of its damping without damper and for the PS coupled with the VI NES, whose parameters were optimized for c_1=452 N·s/m and obtained the values presented in Table 1.

Table 3 summarizes the energy values in numbers and the PS energy reduction in persent.

Table 2

The reduction of the maximum total energy of the PS with different damping c_1 coupled with VI NES whose parameters were optimized for c_1=452 N·s/m. The maximum damper energy E_{2max}

c_1, N·s/m	412	422	432	442	**452**	462	472	482	492
E_{1max}, J, PS without damper	1890	1801	1719	1642	**1571**	1503	1440	1381.3	1326
E_{1max}, J, PS with damper	1119	1041	965.9	892.8	**667.0**	655.3	639.9	625.1	610.8
% reduction of E_{1max}	41	42	44	46	**58**	56	56	55	54
E_{2max}, J	53.9	52.2	80.7	57.2	**135**	46.1	44.7	43.3	42.0
Note	*Bilateral impacts*					*Unilateral impacts against PS only*			

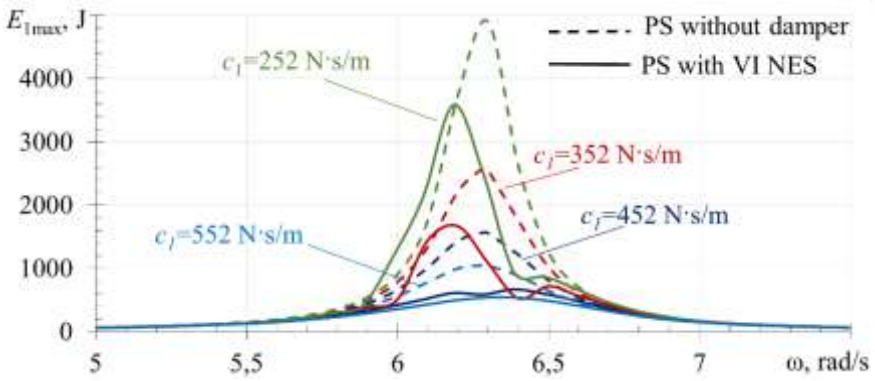

Fig.5. The maximum total mechanical energy of the PS E_{1max} for four values of its damping c_1 without damper (dashed curves) and for the PS coupled with the VI NES, whose parameters were optimized for c_1=452 N·s/m and given in Table 1 (solid curves)

Table 3

The reduction of the maximum total energy of the PS with four different damping c_1 coupled with VI NES whose parameters were optimized for c_1=452 N·s/m. The maximum damper energy E_{2max}

c_1, N·s/m	252	352	**452**	552
E_{1max}, J, PS without damper	5037	2587	**1571**	1054
E_{1max}, J, PS with damper	3589	1664	**667.0**	538.1
% reduction of E_{1max}	29	36	**58**	49
E_{2max}, J	106.4	50.8	**135**	40.5

In [1], the authors note that “energy dissipation is accomplished by three mechanisms: (1) the NES damping, (2) energy loss during NES inelastic impacts and (3) the structural modal damping”. It is important to note that one type of damping can be replaced by another one. In Fig. 5, one can see almost the same effect of both increasing the primary structure damping c_1=452 N·s/m (dashed dark blue curve)and attaching the low-mass VI NES to the primary structure with lower damping c_1=352 N·s/m (solid brown curve). Figs. 6 (a) and (b) demonstrate this effect for two system variants, where the PS with higher damping but without damper and the PS with lower damping but with attached damper provide the same values of its maximum total energy.

How will the damper efficiency and dynamics of the system with attached VI NES change if their parameters are optimized for new values of structural damping?

ISSN 2410-2547
Опір матеріалів і теорія споруд/Strength of Materials and Theory of Structures. 2025. № 114

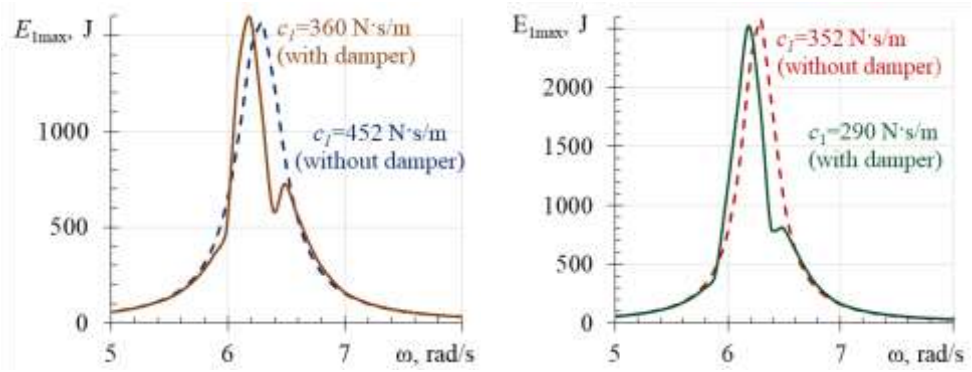

Fig. 6. The damping effect of increasing PS damping c_1 or joining VI NES is the same

3.2. System behavior when optimizing damper parameters with appropriate PS damping

In this section, the SSVI NESs were tuned to the different PS damping, that is, their optimal designs were found for the PS with appropriate damping. After performing optimization procedures separately for each PS damping value, the optimized VI NES parameters were selected as follows (Table 4). Optimization procedures were carried out by tools of standard *Matlab* software using *surf* and *fminsearch* programs.

Table 4

Parameters of VI NESs of mass m_2=20 kg optimized with appropriate PS damping

c_1, N·s/m	k_2, N/m	c_2, N·s/m	C, m	D, m
252	187	26.6	1.36	0.126
352	228	21.7	1.33	0.141
552	229	23.1	0.966	0.170

Table 4 shows that the trend of unusualness for the clearance C and damping coefficient c_2 for lightweight dampers persists; the clearance C is very large and the damping coefficient c_2 is small. Fig. 7, obtained with the *surf* program, confirms the validity of this choice. These plots show the top-down views of the 3D diagrams depicting the relationship between two parameters of SSVI NES with mass m_2=20°kg, when PS damping c_1 =352 N·s/m. The values of the objective function, i.e. the maximum total PS energy E_{1max}, are shown in color. Fig. 7 (a) demonstrates that its lower values depicted in blue and dark blue colors correspond to large values of clearance C. Fig. 7 (b) shows that its lower values depicted in blue and dark blue colors correspond to small values of damper damping c_2.

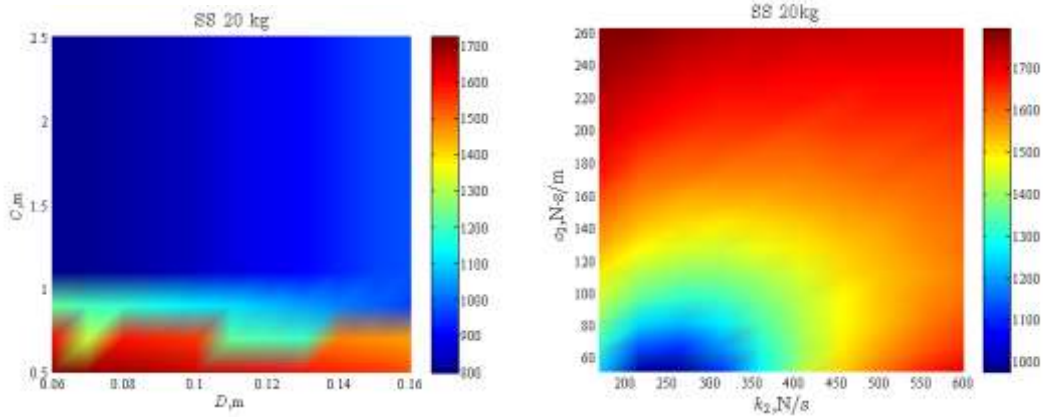

(a) (b)

Fig. 7. The relationship between two parameters of SSVI NES with mass m_2=20 kg, when PS damping c_1=352°N·s/m: (a) between (D – C) k_2=198 N/m, c_2=36.0 N·s/m; (b) between (k_2 – c_2) D=0.11 m, C=0.87 m

The areas of bilateral impacts both directly on the PS and on obstacle are still narrow. In Fig. 8, they are shown in pink color; the areas of the unilateral direct damper impacts on the PS are wider, they are shown in light green color. In the white zones, the motion is shockless and there is no nonlinearity.

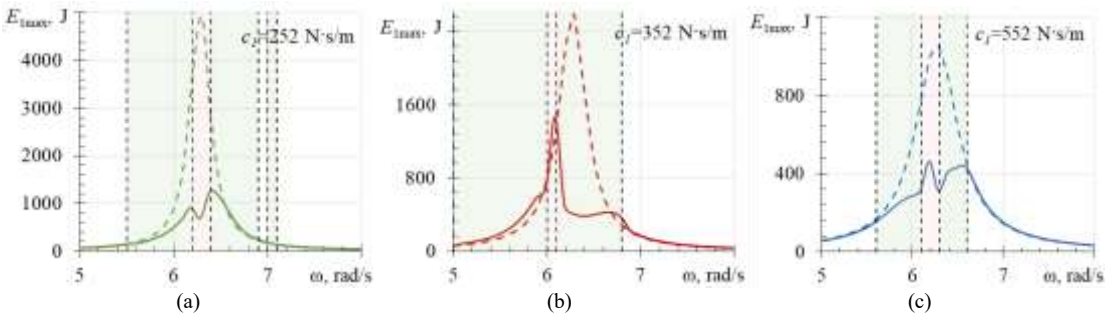

(a) (b) (c)

Fig. 8. The areas of bilateral (pink) and unilateral (light-green) impacts for VI NESs with mass m_2=20 kg, whose parameters were optimized for appropriate PS damping: (a) c_1=252 N·s/m, (b) c_1=352 N·s/m, (c) c_1=552 N·s/m

The damper efficiency is improved when its parameters are optimized at appropriate structural parameters. Table 5 clearly demonstrates this improvement; the lowest green row is given for ease of comparison.

Table 5

The reduction of the maximum total energy for the PS with four different damping coupled with VI NES whose parameters were optimized for appropriate PS damping. The maximum damper energy E_{2max}

c_1, N·s/m	252	352	**452**	552
E_{1max}, J, PSwithout damper	5037	2587	**1571**	1054
E_{1max}, J, PSwith damper	1234	1469	**667.0**	464.0
% reduction of E_{1max}	76	43	**58**	56
% reduction of E_{1max} from Table 3	29	36	**58**	49
E_{2max}, J	198	261	**135**	132

Thus, as we have noted earlier, the low-mass VI NESs (mass ratio 1 and 2 %) have a rather high efficiency in mitigating the primary structure vibrations when their parameters are optimized. However, these parameters acquire unusual “strange” values, namely, very large clearance C and small damping coefficient c_2. In addition, the areas of bilateral damper impacts both directly on the PS and on the obstacle are narrow; the areas of unilateral direct damper impacts on the PS are wider. These phenomena persist when the structural parameters are changed. In particular, Table 4, Table 5 and Fig. 8 clearly demonstrate them when changing the PS damping c_1.

System dynamics with SSVI NES is always complex;there is often an amplitude-modulated response. For example, Fig. 9 shows the amplitude-modulated response of the system at ω=6.38 rad/s, when the PS damping c_1=252 N·s/m and the SSVI NES has parameters optimized for this damping, which are presented in the top row in Table 4. Fig. 9 (a) presents the PS displacements with the upper envelope highlighted in red; its frequency is Ω=0.332015 rad/s. The modulation depth (modulation factor) is m=21 %. Figs.9 (b) and (c) show the contact forces for direct impacts on the PS in blue color (b) and on the obstacle in green color (c). Fig. 9 (d) presents the phase portraits with Poincaré maps in red color for the PS on the left and for the damper on the right. In this plot, the velocity jumps at the impact moments are clearly visible. Fig. 9 (e) presents the Fourier spectrum, in logarithmic scale in inner frame.

ISSN 2410-2547
Опір матеріалів і теорія споруд/Strength of Materials and Theory of Structures. 2025. № 114

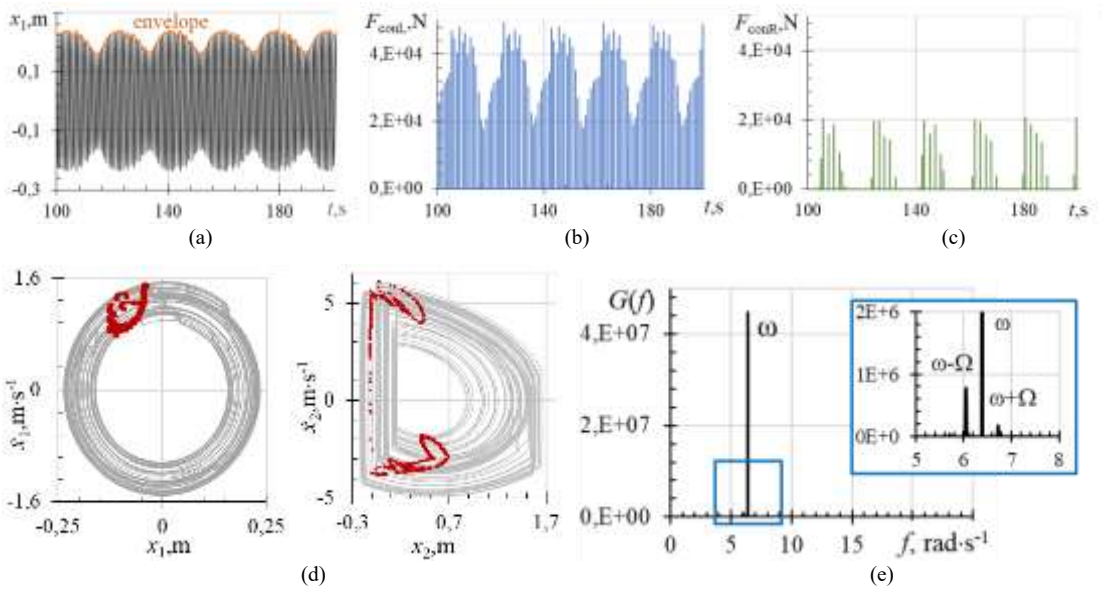

Fig. 9. The amplitude-modulated response of the system at ω=6.38 rad/s, when the PS damping c_1=252 N·s/m and the SSVI NES has parameters optimized for this damping, which are presented in the top row in Table 4. (a) PS displacements with the upper envelope highlighted in red; (b), (c) the contact forces for direct impacts on the PS (b) and on the obstacle (c); (d) the phase portraits with Poincaré maps in red color for the PS on the left and for the damper on the right; (e) the Fourier spectrum

3.3. System behavior when PS is coupled to a linear damper

In the above sections in Figs. 3 and 8, narrow areas of the damper impacts on the obstacle have been shown. If you move the obstacle away and increase the distance between the PS and the damper, i.e., increase the clearance C and distance D, the damper operates as a linear one without any impacts. If we tune it to PS damping c_1=452 N·s/m, i.e., optimize its parameters at this damping value, we get a tuned mass damper (TMD). Optimization of the parameters c_2 and k_2 for the damper with mass m_2=20 kg when D and C are large is performed using the *surf* program from the *Matlab* platform (Fig. 10). The dot in the blue field in this figure defines them as follows:

$$k_2=X=600 \text{ N/m}, \; c_2=Y=52 \text{ N·s/m}.$$

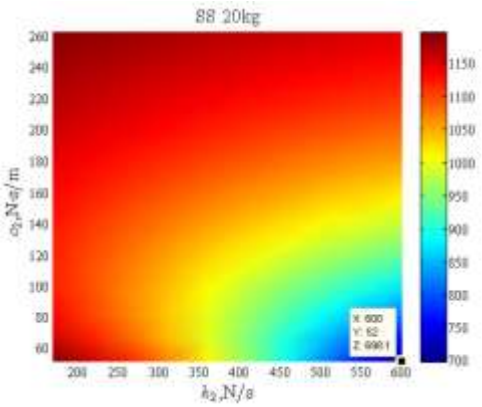

Fig. 10. Finding optimal parameters of linear damper using the *surf* program

The linear damper with these parameters, tuned to PS damping c_1=452 N·s/m, has a sufficiently high efficiency, which is maintained for other PS damping c_1 (Figs. 11, 12).

Fig. 11 (a) is Fig. 4 (a), to which the colored dotted curves were added. They correspond to the PS energy behavior when the TMD is coupled to the PS. The upper dashed curves show the PS energy without damper, the colored solid curves show the PS energy when SSVI NES is coupled to it. Fig. 11 (b) is almost identical to Fig. 4 (b); the colored dotted curves were added, but the colored solid curves were removed because they almost merged. Fig. 12 presents such dependences for the larger values of PS damping c_1.

Figs. 11 and 12 clearly show that the high efficiency of linear damper is maintained over a wide range of PS damping. Table 6 supports this assertion in numbers. The linear TMD, which has no nonlinearity, also takes away some of the PS energy, thereby reducing it; its maximum energy E_{2max} is given in Table°6.

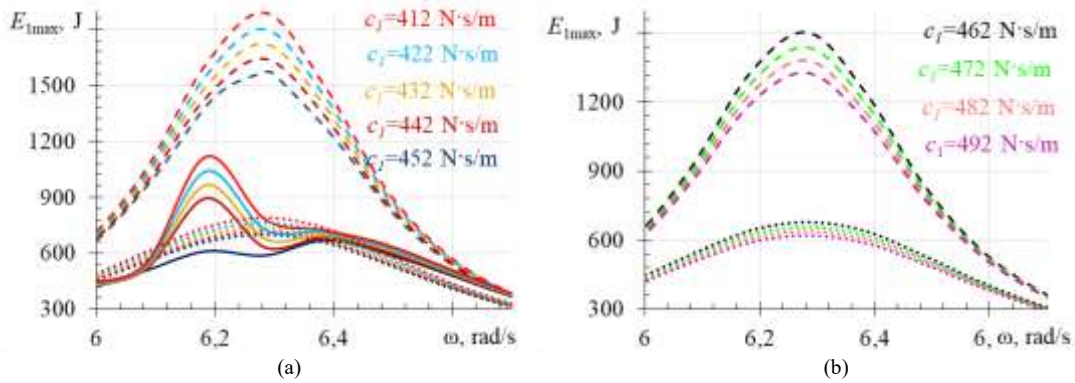

Fig. 11. The reduction of maximum PS energy with attached SSVI NES and TMD when changing the PS damping°c_1: (a) for c_1=412, 422, 432, 442, 452 N·s/m; (b) for c_1=462, 472, 482, 492 N·s/m

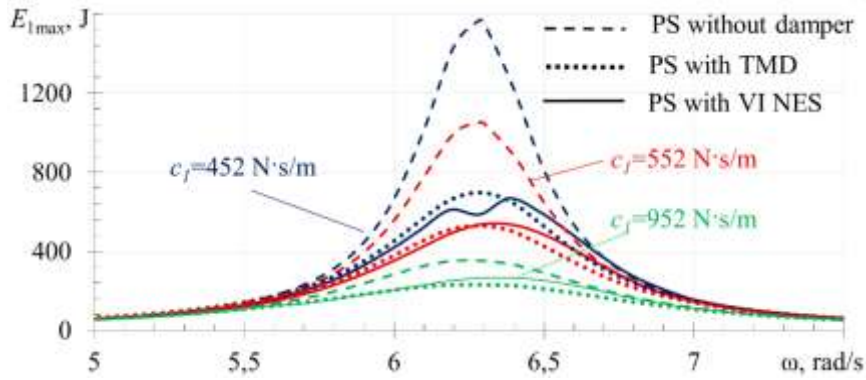

Fig. 12. The reduction of maximum PS energy with attached SSVI NES and TMD when changing the PS damping c_1

Table 6

The reduction of the maximum total energy for the PS coupled with TMD. The maximum damper energy E_{2max}.

c_1, N·s/m	412	422	432	442	**452**	462	472	482	492	552	952
E_{1max}, J, PS without damper	1890	1801	1719	1642	**1571**	1503	1440	1381	1326	1054	354.5
E_{1max}, J, PS with TMD	787.6	763.5	740.5	718.5	**697.5**	677.4	658.1	639.7	622.0	529.9	231.3
% reduction of E_{1max}	58	58	57	56	**56**	55	54	54	53	50	35
E_{2max}, J	64.2	62.3	58.7	56.9	**55.3**	53.7	52.2	50.7	49.2	41.8	18.0

Thus, the system under consideration with certain parameters and harmonic excitation does not demonstrate the advantages of nonlinear vibro-impact damper compared to a tuned linear damperwhen the PS damping is changed.The authors of a very serious review [1] write with reference to an old paper by many reputable authors [16]:" In general, the structural vibration control aims to dissipate excessive vibrational energy from a primary structure using an auxiliary device. Different types of passive damping devices … have been theoretically and experimentally investigated for vibration mitigation in civil structures but no particular damper was found efficient under all circumstances". Consequently, the choice of an effective and reliable damper may be different for different real constructions.

4. Conclusions

In this paper, the effect of varying the structural parameters on the efficiency of single-sided vibro-impact nonlinear energy sinks coupled to a primary structure was studied. The damper efficiency in mitigating the primary structure vibrations and the system behavior when the damping of the primary structure is changed were investigated. The effect of optimizing the damper parameters for each PS damping separately was also studied. The above results allow us to draw following conclusions.

- The efficiency of a damper tuned to a certain PS damping, that is, whose parameters have been optimized at this PS damping, remains sufficiently high over some range of PS damping.
- The efficiency of a damper tuned to a certain PS damping, that is, whose parameters have been optimized at this PS damping, detereorates over a wider range of PS damping.
- Optimizing the damper parameters for appropriate PS damping, i.e., tuning the damper to the appropriate structural parameters, significantly improves their efficiency.
- Coupling the VI NES to the PS has the same effect on the system behavior as increasing the PS damping.
- The parameters of low-mass dampers optimized for different values of structural parameters always acquire unusual “strange” values, namely very large clearance and small damping coefficient

The areas of bilateral damper impacts both directly on the PS and on the obstacle are always narrow.

The areas of unilateral direct impacts only on the PS are wider.

- Dynamics of the system with attached SSVI NES is always complex. The amplitude-modulated responses often occur.
- Tuned mass damper demonstrates the effect of mitigating the PS vibrations in the system under consideration, which is as good as the effect exhibited by the vibro-impact nonlinear energy sink.

REFERENCES

1. Saeed A.S., Abdul Nasar R., Al-Shudeifat M.A. A review on nonlinear energy sinks: designs, analysis and applications of impact and rotary types // Nonlinear Dynamics. – 2022. – T. 111, № 1. – C. 1–37. DOI: 10.1007/s11071-022-08094-y.
2. Saeed A.S., AL-Shudeifat M.A., Cantwell W.J., Vakakis A.F. Two-dimensional nonlinear energy sink for effective passive seismic mitigation // Communications in Nonlinear Science and Numerical Simulation. 2021. Vol. 99. P. 105787. DOI: 10.1016/j.cnsns.2021.105787.
3. Lu Z., Wang Z., Zhou Y., Lu X. Nonlinear dissipative devices in structural vibration control: A review // Journal of Sound and Vibration. – 2018. – T. 423. – C. 18–49. DOI:10.1016/j.jsv.2018.02.052 .
4. Lu Z., Wang Z., Masri S. F., Lu X. Particle impact dampers: Past, present, andfuture // Structural Control and Health Monitoring. – 2017. – T. 25, № 1. – C. e2058. DOI: 10.1002/stc.2058
5. Wang J., Wierschem N. E., Spencer B. F., Lu X. Track nonlinear energy sink for rapid response reduction in building structures // Journal of Engineering Mechanics. – 2015. – T. 141, № 1. DOI: 10.1061/(ASCE)EM.1943-7889.000082
6. Wierschem N. E., Spencer B. F. Jr. Targeted energy transfer using nonlinear energy sinks for the attenuation of transient loads on building structures // Tech. Rep. 045. – Newmark Structural Engineering Laboratory, University of Illinois at Urbana-Champaign, 2015. – Режим доступу: https://www.ideals.illinois.edu/items/89701.
7. Wang Y., Zhang J., Wang W., Wang Z., Hong J., Fang B. Research on the influence of finite contact stiffness on vibration reduction of a vibro-impact nonlinear energy sink system // International Journal of Non-Linear Mechanics. – 2025. – T. 170. – C. 104991. DOI:10.1016/j.ijnonlinmec.2024.104991 .
8. Lizunov P., Pogorelova O., Postnikova T. Comparative Analysis of Performance of Single-sided and Double-sided Vibro-Impact Dampers // NODYCON2025. – Under Review.
9. Lizunov P., Pogorelova O., Postnikova T. Features of different variants for optimal design of vibro-impact nonlinear energy sinks affectingt heir efficiency and dynamics. – 2025. – DOI: 10.2139/ssrn.5179053.
10. Wierschem N. E., Hubbard S. A., Luo J., Fahnestock L. A., Spencer B. F., McFarland D. M., Quinn D. D., Vakakis A. F., Bergman L. A. Response attenuation in a large-scale structure subjected to blast excitation utilizing a system of essentially nonlinear vibration absorbers // Journal of Sound and Vibration. – 2017. – T. 389. – C. 52–72. DOI: 10.1016/j.jsv.2016.11.003 .
11. Li T., Seguy S., Berlioz A. On the dynamics around targeted energy transfer for vibro-impact nonlinear energy sink // Nonlinear Dynamics. – 2016. – T. 87, № 3. – C. 1453–1466. DOI: 10.1007/s11071-016-3127-0.
12. AL-Shudeifat M. A., Wierschem N., Quinn D. D., Vakakis A. F., Bergman L. A., Spencer B. F. Numerical and experimental investigation of a highly effective single-sided vibro-impact non-linear energy sink for shock mitigation // International Journal of Non-Linear Mechanics. – 2013. – T. 52. – C. 96–109. DOI: 10.1016/j.ijnonlinmec.2013.02.004.
13. Johnson K. L. Contact Mechanics. – 1985. DOI: 10.1017/cbo9781139171731 .
14. Bazhenov V., Pogorelova O., Postnikova T. Crisis-Induced Intermittency and Other Nonlinear Dynamics Phenomena in Vibro-impact System with Soft Impact // Non linear Mechanics of Complex Structures. – 2021. – C. 185–203. DOI: 10.1007/978-3-030-75890-5_11.

15. Lizunov P., Pogorelova O., Postnikova T. Optimization of a vibro-impactdamperdesignusing MATLAB tools // Strength of Materials and Theory of Structures. – 2024. – Issue 112. – С. 3–18. DOI: 10.32347/2410-2547.2024.112.3-18.
16. Housner G. W., Bergman L. A., Caughey T. K., Chassiakos A. G., Claus R. O., Masri S. F., Skelton R. E., Soong T. T., Spencer B. F., Yao J. T. P. Structural control: past, present, and future // Journal of Engineering Mechanics. – 1997. – Т. 123, № 9. – С. 897–971. DOI: 10.1061/(ASCE)0733-9399(1997)123:9(897).

Стаття надійшла 30.03.2025

Лізунов П.П., Погорелова О.С., Постнікова Т.Г.

НАЛАШТУВАННЯ ВІБРОУДАРНИХ НЕЛІНІЙНИХ ПОГЛИНАЧІВ ЕНЕРГІЇ ПРИ ЗМІНІ КОНСТРУКТИВНИХ ПАРАМЕТРІВ. ЧАСТИНА 1

У цій статті досліджується ефективність віброударного нелінійного поглинача енергії (віброударного демпфера) у гасінні коливань первинної структури, тобто у зменшенні її повної механічної енергії. Первинна конструкція являє собою лінійний осцілятор, який утворює сильно нелінійну віброударну систему, коли до нього приєднується віброударний демпфер. При налаштуванні демпфера на певне значення конструктивного параметра, зокрема, демпфування первинної структури, його досить висока ефективність зберігається в деякому діапазоні цього параметра і погіршується в більш широкому діапазоні. Тоді налаштування конструкції демпфера на відповідне значення демпфування первинної структури дозволяє суттєво підвищити його ефективність. Процедури оптимізації здійснюються засобами стандартного програмного забезпечення *Matlab*. Однак оптимізовані параметри мало масового демпфера набувають незвичних «дивних» значень, а саме: дуже великий зазор і малий коефіцієнт демпфування. Крім того, зони двобічних ударів демпфера як безпосередньо об основну конструкцію, так і о перешкоду є вузькими, а зони однобічних прямих ударів демпфера об основну конструкцію є ширшими. Ці явища, що спостерігалися в наших попередніх роботах для одного конкретного значення демпфування первинної структури, зберігаються і для різних його значень. Також показано, як установка VI NES може замінити додаткове демпфування ПС. Динаміка системи з однобічним віброударним нелінійним поглиначем енергії, зв'язаним з первинною структурою, завжди складна, часто виникають амплітудно-модульовані відгуки системи. Показано характеристики такого режиму, а саме: графік переміщень з верхньою огинаючою, ліву та праву контактні сили, фазові портрети з картами Пуанкаре та спектри Фур'є. Моделювання удару з використанням нелінійної контактної сили Герца відповідно до його квазістатичної теорії дозволяє розрахувати контактні сили удару, врахувати і оптимізувати характеристики поверхонь, що стикаються.

Якісні рисунки і таблиці супроводжують великий обсяг чисельних експериментів.

Ключові слова: нелінійний поглинач енергії, демпфер, віброудар, оптимізовані параметри, ефективність, двосторонні удари.

Lizunov P.P., Pogorelova O.S., Postnikova T.G.

TUNING OF VIBRO-IMPACT NONLINEAR ENERGY SINKS UNDER CHANGING STRUCTURAL PARAMETERS. PART 1

This paper studies the efficiency of vibro-impact nonlinear energy sink, that is, vibro-impact damper, in mitigating the primary structure vibrations, i.e., in reducing its total mechanical energy. The primary structure is a linear oscillator that forms a strongly nonlinear vibro-impact system when a vibro-impact damper is coupled to it. When the damper is tuned to a certain value of a structural parameter, in particular, the primary structure damping, its sufficiently high efficiency is maintained in some this parameter range and deteriorates in a wider range. Then tuning the damper design to the appropriate value of the primary structure damping allows to significantly improve its efficiency. Optimization procedures are carried out by the tools of standard software *Matlab*. However, the optimized parameters of the low-mass damper acquire unusual “strange” values, namely, very large clearance and small damping coefficient. In addition, the areas of bilateral damper impacts both directly on the primary structure and on the obstacle are narrow; the areas of unilateral direct damper impacts on the primary structure are wider. These phenomena, observed in our previous works for one particular value of the primary structure damping, persist for its different values. It is also shown how a VI NES attachment can replace the additional PS damping. The system dynamics with the single-sided vibro-impact nonlinear energy sink coupled to the primary structure is always complex; the amplitude-modulated responses are often occur. The characteristics of such a regime are shown, namely, the time history of displacements with upper envelope, left and right contact forces, the phase portraits with Poincaré maps, and Fourier spectra. Modeling the impact using the nonlinear Hertz’s contact force in accordance with his quasi-static theory allows us to calculate the impact contact forces, take into account and optimize the characteristics of the colliding surfaces.

Qualitative figures and tables accompany a large volume of numerical experiments.

Keywords: nonlinear energy sink, damper, vibro-impact, optimized parameters, efficiency, bilateral impacts.

УДК 539.3
Лізунов П.П., Погорелова О.С., Постнікова Т.Г. **Налаштування віброударних нелінійних поглиначів енергії при зміні конструктивних параметрів. Частина 1** // Опір матеріалів і теорія споруд: наук.-тех. збірн. – К.: КНУБА. 2025. – Вип. 114. – С. 11-22. – Англ.

Показано, як налаштування віброударних нелінійних поглиначів енергії на відповідні конструктивні параметри може підвищити їхню ефективність у ширшому діапазоні цих параметрів. Незвичні «дивні» значення оптимізованих параметрів для мало масивних демпферів (дуже великий кліренс і малий коефіцієнт демпфування) і вузькі області двосторонніх ударів зберігаються також при різних значеннях конструктивних параметрів.
Таб. 6. Іл. 12. Бібліогр. 16 назв.

ISSN 2410-2547
Опір матеріалів і теорія споруд/Strength of Materials and Theory of Structures. 2025. № 114

UDC 539.3
Lizunov P.P., Pogorelova O.S., Postnikova T.G. **Tuning of vibro-impact nonlinear energy sinks under changing structural parameters. Part 1** // Strength of Materials and Theory of Structures: Scientific-and-technical collected articles. – K.: KNUBA. 2025. – Issue 114. – P. 11-22.
It is show how tuning of vibro-impact nonlinear energy sinks to appropriate structural parameters can improve their efficiency over wider range of these parameters. Unusual "strange" values of optimized parameters for low-mass dampers (very large clearance and small damping coefficient) and narrow areas of bilateral impacts persist also at different structural parameter values.
Tabl. 6. Figs. 12. Refs. 16.

Автор (науковий ступінь, вчене звання, посада): доктор технічних наук, професор, завідувач кафедри будівельної механіки КНУБА, директор НДІ будівельної механіки ЛІЗУНОВ Петро Петрович
Адреса робоча: 03680 Україна, м. Київ, проспект Повітряних Сил 31, Київський національний університет будівництва і архітектури
Робочий тел.: +38(044) 245-48-29
Мобільний тел.: +38(067)921-70-05
E-mail: lizunov@knuba.edu.ua
ORCIDID: http://orcid.org/0000-0003-2924-3025

Автор (науковий ступінь, вчене звання, посада): кандидат фізико-математичних наук, старший науковий співробітник, провідний науковий співробітник НДІ будівельної механіки ПОГОРЕЛОВА Ольга Семенівна
Адреса робоча: 03680 Україна, м. Київ, проспект Повітряних Сил 31, Київський національний університет будівництва і архітектури
Робочий тел.: +38(044) 245-48-29
Мобільний тел.: +38(067) 606-03-00
E-mail: pogos13@ukr.net
ORCID ID: http://orcid.org/0000-0002-5522-3995

Автор (науковий ступінь, вчене звання, посада): кандидат технічних наук, старший науковий співробітник, провідний науковий співробітник НДІ будівельної механіки ПОСТНІКОВА Тетяна Георгіївна
Адреса робоча: 03680 Україна, м. Київ, проспект Повітряних Сил 31, Київський національний університет будівництва і архітектури
Робочий тел.: +38(044) 245-48-29
Мобільний тел.: +38(050) 353-47-19
E-mail: postnikova.tg@knuba.edu.ua
ORCID ID: https://orcid.org/0000-0002-6677-4127